AIAA Journal
Vol. 46, No. 10, October 2008

Instability of Adverse-Pressure-Gradient Boundary Layers with Suction

P. J. D. Roberts* and J. M. Floryan†
University of Western Ontario, London, Ontario N6A 5B9, Canada

DOI: 10.2514/1.32624

Boundary layers exposed to an adverse pressure gradient are known to be very unstable with respect to traveling wave instability. This instability can be eliminated through the application of wall suction. It is shown that when suction distribution is not uniform, another type of instability may occur, giving rise to streamwise vortices. It is further shown that an increase of uniform suction is not an effective method for control of this instability. Finally, it is shown that nonuniformities of surface blowing can induce similar vortex-type instability.

Nomenclature

c_n	=	arbitrary constants
D	=	derivative operator, d/dy
F	=	similarity function in the Falkner–Skan equation
$\bar{G}_m$	=	disturbance amplitude field, $(g_u^{(m)}, g_w^{(m)}, g_v^{(m)})$
$K_u^{(m)}, K_w^{(m)}, K_v^{(m)}$	=	elements of the linear stability operator
k_m, t_m	=	elements of the linear stability operator
$L_u^{(m)}, L_w^{(m)}, L_v^{(m)}$	=	elements of the linear stability operator
$M_u^{(m)}, M_w^{(m)}, M_v^{(m)}$	=	elements of the linear stability operator
$N_u^{(m)}, N_w^{(m)}, N_v^{(m)}$	=	elements of the linear stability operator
Re	=	Reynolds number
Re_s	=	suction Reynolds number
S	=	amplitude of suction nonuniformity
$S^{(m)}, T^{(m)}$	=	elements of the linear stability operator
U	=	velocity at boundary-layer edge
$\hat{u}_1, \hat{v}_1$	=	flow modification amplitude functions
$\bar{u}_3$	=	amplitude function of the disturbance velocity field
$\bar{v}$	=	total velocity field in the stability analysis
$\bar{v}_0, p_0$	=	reference flow velocity and pressure fields, (u_0, w_0, v_0)
$\bar{v}_1, p_1$	=	velocity and pressure modifications due to wall suction, $(u_1, 0, v_1)$
$\bar{v}_2, p_2$	=	mean modified flow and pressure fields
$\bar{v}_3$	=	disturbance velocity field
$\bar{w}_3$	=	amplitude function of the disturbance velocity field
$\bar{x}$	=	position vector (x, z, y)
y	=	wall-normal coordinate made dimensionless with δ^*
α	=	streamwise wave number of flow disturbance and/or wall suction
β	=	pressure gradient parameter in the Falkner–Skan equation
γ	=	suction parameter in the Falkner–Skan equation
δ	=	Floquet exponent
δ^*	=	dimensional displacement thickness
η	=	similarity variable in the Falkner–Skan equation
λ_n	=	roots of the characteristic equation in the solution describing flow modifications outside of the boundary layer
μ	=	spanwise wave number of flow disturbance
σ	=	complex amplification rate, $\sigma_r + i\sigma_i$
Φ	=	stream function amplitude function
ψ	=	stream function of the mean modified flow
$\bar{\omega}$	=	total vorticity field in the stability analysis
$\bar{\omega}_2$	=	vorticity field of the modified mean flow
$\bar{\omega}_3$	=	disturbance vorticity field
$*$	=	dimensional quantities

Received 5 June 2007; revision received 22 November 2007; accepted for publication 24 December 2007.

*Graduate Student, Department of Mechanical and Materials Engineering; currently, Sharcnet, Canada.
†Professor, Department of Mechanical and Materials Engineering.

I. Introduction

Boundary layers with an adverse pressure gradient are known to be highly unstable due to the appearance of an inflection point in the streamwise velocity distribution. The instability severely limits the extent of laminar flow in the pressure recovery zone of laminar-flow airfoils. The flow in this zone can be stabilized by the application of wall suction [1]. A number of investigations have been devoted to the determination of the proper magnitude and distribution of such suction [2]. Because real suction systems can produce the required suction distribution only with some approximation, the question arises how the possible deviations in the desired suction distribution may affect the flow [3]. If such deviations have a negative influence, one is interested in the determination of the additional net suction required to stabilize the flow.

The laminar–turbulent transition process in boundary layers results from the growth of small disturbances. This growth is described by the classical linearized operator and can have two forms. The asymptotic growth (as $t \to \infty$) is described by the eigenvalues of this operator. The flow is considered stable if there are no unstable eigenvalues. Even if all eigenvalues are stable, disturbances can be subject to an initial growth, so-called transient growth, due to the interdependence of various linear modes associated with the nonnormality of the operator. The transient growth may be sufficient to bring disturbances to the level at which they can trigger a bypass transition. Although these issues are well understood in the case of ideal parallel flows [4], very little is known about them even in the case of slightly different flows.

The asymptotic instability in boundary layers has the form of traveling wave instability. The critical disturbances have the form of two-dimensional waves traveling in the downstream direction and are frequently referred to as the Tollmien-Schlichting (TS) waves. Reed et al. [5] provide a good description of the various processes associated with this instability.

The question of change in the characteristics of asymptotic instability resulting from the presence of suction nonuniformities can

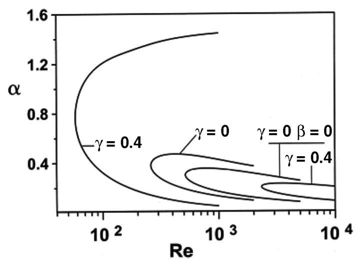

Fig. 1 Neutral stability curves describing two-dimensional traveling wave (TS) instability in the Blasius boundary layer and in the Falkner–Skan boundary layers with pressure gradient $\beta = -0.07$ and levels of suction $\gamma = -0.4, 0, +0.4$.

be addressed by selecting Falkner–Skan flows as generic representatives of boundary layers with adverse pressure gradient. The Falkner–Skan flows with uniform suction represent the reference case, and the off-design conditions are represented by the addition of suction nonuniformities. It is useful to summarize the stability characteristics of such reference flows. The Blasius boundary layer becomes unstable at $Re_{\mathrm{cr}} \approx 520$, where Re denotes the Reynolds number based on the displacement thickness (Fig. 1). When the Falkner–Skan pressure parameter decreases from $\beta = 0$ to -0.07, the critical Reynolds number decreases from $Re_{\mathrm{cr}} \approx 520$ to ≈ 261 (see Fig. 1). Application of uniform blowing corresponding to the suction parameter $\gamma = +0.4$ reduces the critical Reynolds number to $Re_{\mathrm{cr}} \approx 58.2$, whereas application of uniform suction corresponding to $\gamma = -0.4$ increases the critical Reynolds number to $Re_{\mathrm{cr}} \approx 2350$. These results show that uniform suction has a very strong stabilizing effect on traveling wave instability.

Transient growth in boundary layers has attracted a lot of attention more recently [6,7]. The available results indicate that the most significant growth is associated with streamwise vortices. This growth is reduced by applying a favorable pressure gradient, when compared with the boundary layer with a constant pressure [8,9]. There are indications that wall suction is also effective at reducing the transient growth of disturbances [10].

The effect of suction nonuniformities was studied for the first time by Floryan [11], who showed that such nonuniformities can produce an instability that gives rise to streamwise vortices. Floryan [12] analyzed the stability of the Blasius boundary layer in the presence of infinitesimally small suction nonuniformities and concluded that such nonuniformities may interfere with the TS waves only if they have the form of waves that are in near resonance with the neutral TS waves. Roberts et al. [13] considered small but finite stationary suction nonuniformities and concluded that they have a rather small effect on the TS waves. They also showed that these nonuniformities induce a vortex-type instability that cannot be effectively controlled by increasing the level of uniform suction. Roberts and Floryan [14] studied boundary layers with a favorable pressure gradient and concluded that the vortex instability changes very little with the pressure gradient and thus it may represent the dominant instability in such flows.

The suction nonuniformities can be introduced intentionally as a technique for stabilization of TS waves using the wave-cancellation principle [15]. Although such suction may lead to the reduction/elimination of the undesired TS waves, it may induce its own instabilities [11]. One should note that the wave-cancellation process is never ideal and it always results in the scattering of additional waves [16]. This process has not been studied in the case of boundary layers.

The appearance of an adverse pressure gradient very often signals impending flow separation. Such separation can be delayed if additional mixing, resulting in the introduction of transverse momentum transport, can be created. This is typically achieved by intentionally switching the flow to its turbulent form. The occurrence of a vortex-type instability offers an alternative, provided that the instability can be induced in a controlled manner and the associated mixing process is sufficiently intense. In this sense, the suction nonuniformities can be viewed as a tool for flow control. As a result, one is interested in identifying the optimal properties of suction distribution (i.e., the form of the "smallest" suction that produces the "largest" changes in the flow). A very large range of flow responses can be achieved by taking advantage of the near-resonant and/or forced types of responses [16]. A properly selected suction may force the flow system through its stability limit [11], potentially resulting in a laminar form of the flow, which is more resistant to separation.

Distributed surface suction can be viewed as an analog of distributed surface roughness. It has been shown in the case of channel flow that the flow instability caused by such suction is qualitatively similar to flow instabilities caused by surface corrugation [11,17]. Analysis of the stability of decelerated boundary layers modified by nonuniform surface suction may thus offer an insight into the dynamics of such flows over rough surfaces.

The main objective of the present work is the determination of the linear stability characteristics of boundary layers with an adverse pressure gradient in the presence of suction nonuniformities and how these characteristics change in response to an increase in the average level of suction. The focus is on the asymptotic instability ($t \to \infty$); a normal mode approach is used and the problem is posed as an eigenvalue problem. The present work can be viewed as an extension of the work described in [13] on decelerating boundary layers. The following presentation is organized as follows. Section II describes the reference flow (i.e., the Falkner–Skan boundary layer). Section III describes flow modifications generated by nonuniform wall suction. Section IV is devoted to the analysis of linear stability of the modified flow. Section V provides a discussion of the results. Section VI gives a summary of the main conclusions.

II. Reference Flow

Consider flow over a semi-infinite flat plate overlapping with the positive x axis, as shown in Fig. 2. In the absence of suction nonuniformities, the fluid motion is described by

$$\bar{v}_0(\bar{x}, t) = (u_0, w_0, v_0) = (\mathrm{d}F/\mathrm{d}\eta,\ 0,\ 0), \qquad P_0(\bar{x}, t) = p_0(x) \tag{1}$$

where the function F is described by the Falkner–Skan equation in the form

$$\begin{aligned} &\mathrm{d}^3F/\mathrm{d}^3\eta + F\,\mathrm{d}^2F/\mathrm{d}\eta^2 - \gamma\,\mathrm{d}^2F/\mathrm{d}\eta^2 + \beta[1-(\mathrm{d}^2F/\mathrm{d}\eta^2)^2] = 0,\\ &F = \mathrm{d}F/\mathrm{d}\eta = 0 \quad \text{at } \eta = 0, \qquad \mathrm{d}F/\mathrm{d}\eta \to 1 \quad \text{as } \eta \to \infty \end{aligned} \tag{2}$$

where η stands for the usual similarity variable, negative β corresponds to the unfavorable pressure gradient, and negative (positive) γ describes the wall suction (blowing). The effects of boundary-layer growth are neglected. There is experimental evidence suggesting that these effects are not important except in the case of high-frequency disturbances [18]. Figure 3 illustrates distributions of $u_0(y)$ for the Blasius boundary layer as well as for the decelerated boundary layer with $\beta = -0.07$ for three levels of suction/blowing ($\gamma = -0.4,\ 0,\ +0.4$). The distance normal to the plate, y, is scaled using the displacement thickness δ^*, defined as

$$\delta^* = \int_0^\infty (1 - u_0^*/U^*)\,\mathrm{d}y^*$$

where U stands for the velocity at the edge of the boundary layer and asterisks denote dimensional quantities. The displacement thickness δ^* is used as the length scale in the rest of this paper.

III. Boundary Layer with Suction Nonuniformities

In this section, we shall consider flow modifications generated by suction nonuniformities. The magnitude of the nonuniformities of interest is such that a linear model provides a sufficiently accurate description of the flow [11]. It is thus sufficient to represent nonuniformities in terms of a Fourier expansion and to analyze the effects of each mode separately. Accordingly, at the wall, we apply suction in the form

$$u_1(x, 0) = 0, \qquad v_1(s, 0) = 0.5Se^{i\alpha x} + \mathrm{CC} \tag{3}$$

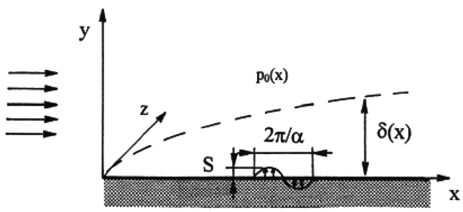

Fig. 2 Sketch of the flow domain.

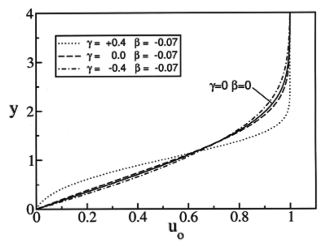

Fig. 3 Distribution of the streamwise velocity component $u_0(y)$ in the Falkner–Skan boundary layer with pressure parameter $\beta = -0.07$ and levels of suction $\gamma = -0.4$, 0, +0.4. The velocity distribution of the Blasius boundary layer ($\beta = 0$ and $\gamma = 0$) is given for reference purposes.

where S is real and denotes suction amplitude, α is the suction wave number, CC stands for the complex conjugate, and i denotes the imaginary unit. The mean modified flowfield may be represented as

$$\bar{v}_2(\bar{x}) = \bar{v}_0(\bar{x}) + \bar{v}_1(\bar{x}) = [u_0(y), 0, 0] + [u_1(x, y), 0, v_1(x, y)],$$
$$p_2(\bar{x}) = p_0(x) + p_1(x, y) \tag{4}$$

where $\bar{v}_1$ and p_1 are velocity and pressure modifications due to the presence of wall suction and the wall-normal velocity component of the unmodified flow was neglected. Substituting Eq. (4) into the two-dimensional Navier–Stokes and continuity equations, eliminating pressure, linearizing the resulting equations for small suction amplitudes S, subtracting the undisturbed flow quantities, introducing a stream function in the form of $u_1 = \partial\psi/\partial y$ and $v_1 = -\partial\psi/\partial x$, and assuming the solution to be in the form

$$\psi(x, y) = \Phi(y)e^{i\alpha x} + \mathrm{CC}, \qquad u_1(x, y) = \hat{u}_1(y)e^{i\alpha x} + \mathrm{CC}$$
$$v_1(x, y) = \hat{v}_1(y)e^{i\alpha x} + \mathrm{CC} \tag{5}$$

leads to the following problem to be solved numerically:

$$D^4\Phi + (-2\alpha^2 - i\alpha Re u_0)D^2\Phi + (\alpha^4 + i\alpha^3 Re u_0 + i\alpha D^2 u_0)\Phi = 0 \tag{6a}$$

$$\Phi = iS/2\alpha, \qquad D\Phi = 0 \quad \text{at } y = 0 \tag{6b}$$

$$\Phi \to 0, \qquad D\Phi \to 0 \quad \text{as } y \to \infty \tag{6c}$$

where Re stands for the Reynolds number based on the displacement thickness and $D = \mathrm{d}/\mathrm{d}y$.

The rate at which flow modifications decay as $y \to \infty$ can be deduced by noting that u_0 becomes constant as $y \to \infty$ and coefficients in Eq. (6a) become constant. The solution outside the boundary layer takes the form

$$\Phi = \sum_{n=1}^{n=4} c_n e^{\lambda_n y} \tag{7}$$

where c_n are arbitrary constants and λ_n are roots of the characteristic equation and have the form

$$\lambda_1 = \alpha, \qquad \lambda_2 = \sqrt{\alpha^2 + iRe\alpha}, \qquad \lambda_3 = -\lambda_1, \qquad \lambda_4 = -\lambda_2 \tag{8}$$

Because real parts of $\lambda_{1,2}$ are positive, the constants $c_{1,2}$ must be zero for flow modifications to vanish far away from the wall.

The problem was solved using two methods. The first method takes advantage of the availability of an analytical solution (7) outside the boundary layer. The second method involves mapping of the half-infinite domain $y \in [0, \infty]$ into a strip $Y \in [0, 1]$ using transformation $Y = \exp(-y/y_0)$. The transformed equations are discretized using a spectral Chebyshev Tau method [19]. Both methods and their testing are described in [13]. The same testing procedures were used in the present work.

IV. Linear Stability of the Modified Flow

This section considers three-dimensional linear stability of boundary-layer flow modified by nonuniform wall suction. The basic state has a spatial structure associated with suction nonuniformities that has to be accounted for in the analysis.

The problem formulation is analogous to that given by Floryan [11]. The following presentation is limited to a short outline. The analysis begins with the governing equations in the form of vorticity transport and continuity equations:

$$\partial\bar{\omega}/\partial t - (\bar{\omega} \cdot \nabla)\bar{v} + (\bar{v} \cdot \nabla)\bar{\omega} = Re^{-1}\nabla^2\bar{\omega} \tag{9a}$$

$$\nabla \cdot \bar{v} = 0 \tag{9b}$$

$$\bar{\omega} = \nabla \times \bar{v} \tag{9c}$$

Unsteady three-dimensional disturbances are superimposed on the mean part in the form

$$\bar{\omega} = \bar{\omega}_2(x, y) + \bar{\omega}_3(x, z, y, t), \qquad \bar{v} = \bar{v}_2(x, y) + \bar{v}_3(x, z, y, t) \tag{10}$$

where subscripts 2 and 3 refer to the mean flow and the disturbance field, respectively. The assumed form [Eq. (10)] of the flow is substituted into the governing Eqs. (9), the mean part is subtracted, and the equations are linearized. The resulting linear disturbance equations have the form

$$\partial\bar{\omega}_3/\partial t + (\bar{v}_2 \cdot \nabla)\bar{\omega}_3 - (\bar{\omega}_3 \cdot \nabla)\bar{v}_2 + (\bar{v}_3 \cdot \nabla)\bar{\omega}_2 - (\bar{\omega}_2 \cdot \nabla)\bar{v}_3 = Re^{-1}\nabla^2\bar{\omega}_3 \tag{11a}$$

$$\nabla \cdot \bar{v}_3 = 0 \tag{11b}$$

$$\bar{\omega}_3 = \nabla \times \bar{v}_3 \tag{11c}$$

The mean flow is assumed to have the form

$$\bar{v}_2(\bar{x}, t) = [u_0(y), 0, 0] + \{[\hat{u}_1(y), 0, \hat{v}_1(y)]e^{i\alpha x} + \mathrm{CC}\} \tag{12}$$

where $\hat{u}_1$ and $\hat{v}_1$ represent solutions of problems (5) and (6).

The disturbance equations have coefficients that are functions of x and y only, and thus the solution can be written in the form

$$\bar{v}_3(x, z, y, t) = \bar{u}_3(x, y)e^{i(-\sigma t + \mu z)} + \mathrm{CC} \tag{13}$$

The exponent μ is real and accounts for the spanwise periodicity of the disturbance field. The exponent σ is assumed to be complex, and its imaginary and real parts describe the rate of growth and the frequency of the disturbances, respectively.

Because the coefficients of the disturbance equations are periodic in x with periodicity $2\pi/\alpha$, $\bar{u}_3$ is written, following the Floquet theory [20], as

$$\bar{u}_3(x, y) = e^{i\delta x}\bar{w}_3(x, y) = e^{i\delta x}\sum_{m=-\infty}^{m=+\infty} \bar{G}_m(y)e^{im\alpha x} \tag{14}$$

where $\bar{w}_3$ is periodic in x with the same periodicity $2\pi/\alpha$, and δ is referred to as the Floquet exponent. The first equation follows from the Floquet theory, whereas the second expresses the Fourier mode decomposition. Our interest is in the temporal stability theory and thus δ is assumed to be real. The final form of the disturbance velocity vector is written as

$$\bar{v}_3(x, z, y, t) = \sum_{m=-\infty}^{m=+\infty} [g_u^{(m)}(y), g_w^{(m)}(y), g_v^{(m)}(y)] e^{i[(\delta+m\alpha)x+\mu z-\sigma t]} + \mathrm{CC} \tag{15}$$

Substitution of Eqs. (12) and (15) into the disturbance equations (11) and separation of the Fourier components results in an infinite system of linear differential equations governing $g_u^{(m)}$, $g_w^{(m)}$, and $g_v^{(m)}$, where $m \in (-\infty, +\infty)$. An explicit form of these equations is given in the Appendix. The disturbance equations are supplemented by the homogeneous boundary conditions, resulting in an eigenvalue problem. This problem was solved using the same spectral method as described in [13] and thus its description will not be repeated here.

V. Discussion of Results

A. Boundary Layer Without Uniform Suction ($\gamma = 0$)

We shall begin our discussion by describing changes in the flow induced by periodic suction nonuniformities (with zero net mass flux). These changes include flow modifications induced directly by the nonuniformities as well as changes in the stability properties of the flow. All presented results were obtained for a boundary layer with pressure parameter $\beta = -0.07$.

Forms of velocity modifications induced by suction nonuniformities are illustrated in Figs. 4 and 5. Results displayed in Fig. 4 demonstrate that flow modifications do not change very rapidly as a function of Reynolds number. In contrast, Fig. 5 indicates a strong variation of flow modifications with suction wave number α.

The stability analysis uses the temporal linear theory and is limited to disturbances that have the same streamwise periodicity as suction nonuniformities. Accordingly, the Floquet exponent δ is set to zero and the exponent σ is assumed to be complex. The rate of growth of disturbances is given by $\mathrm{Im}(\sigma)$.

It is known that in the case of parallel flow approximation, two-dimensional Tollmien–Schlichting (TS) waves determine the critical stability conditions. The addition of suction nonuniformities may alter stability characteristics either through a modification of the properties of the TS waves or through creation of a new instability. Floryan [11] identified one such new instability and provided a preliminary discussion of its characteristics. This particular instability gives rise to disturbances in the form of streamwise spatially modulated vortices [the dominant mode corresponds to $m = 0$ in Eq. (15)] and is completely attributable to suction nonuniformities. These vortices do not propagate [i.e., $\mathrm{Re}(\sigma) = 0$]. We shall now discuss the properties of this instability in details.

1. *Instability in the Form of Streamwise Vortices*

Figure 6 displays the amplification rates of streamwise vortices induced by suction nonuniformities for $Re = 10^3$ and 2×10^3. This instability occurs at flow Reynolds numbers at which TS waves are also unstable (compare Figs. 1 and 6). It may be noted that the values of Reynolds number and suction nonuniformity amplitude S required to induce this instability are similar to those required to induce the same instability in boundary layers without pressure gradient [13] and with favorable pressure gradient [14]. Figure 6 also shows that the range of suction wave numbers α, which gives rise to the instability, exists as a band bounded from below and from above. For each wave number α, a finite band of unstable vortex wave numbers μ bounded from above and from below is found. It can also be seen that the vortex amplification rates, as well as the range of α and μ, increase with increasing values of Reynolds number. At the same time, the maximum amplification rate shifts toward larger α.

Figure 7 demonstrates that amplification rates increase when either 1) the suction nonuniformity amplitude is increased or 2) the Reynolds number is increased. The former can easily be seen by considering constant Reynolds number and examining how amplification rates change for different levels of suction amplitude, whereas the latter can be seen by considering constant suction amplitude and examining how amplification rates change for different levels of the Reynolds number.

Figure 8 shows the flow response as a function of both the suction amplitude and Reynolds number being changed in such a way that the suction Reynolds number, defined as $Re_s = S \times Re$, remains constant. For each level of Re_s considered, the amplification rate appears to reach an asymptotic value as the Reynolds number is increased. As a result, it may be possible to define a critical suction Reynolds number that guarantees flow stability in the range of parameters considered.

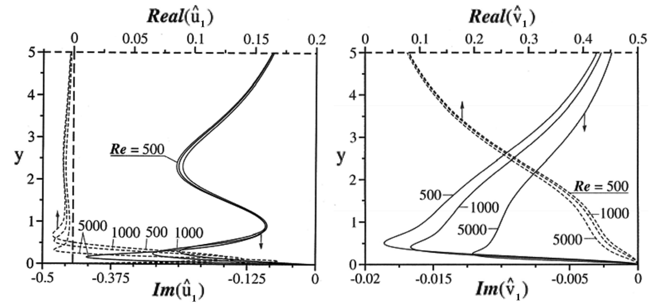

a) b)

Fig. 4 Flow modifications induced by the nonuniform suction with the wave number $\alpha = 0.5$ for different values of Reynolds numbers: a) $\hat{u}_1(y)$ and b) $\hat{v}_1(y)$. Solid and dashed lines represent imaginary and real parts, respectively. All results are normalized with $S = 1$. The presented results are for the Falkner–Skan boundary layer with $\beta = -0.07$ and $\gamma = 0$.

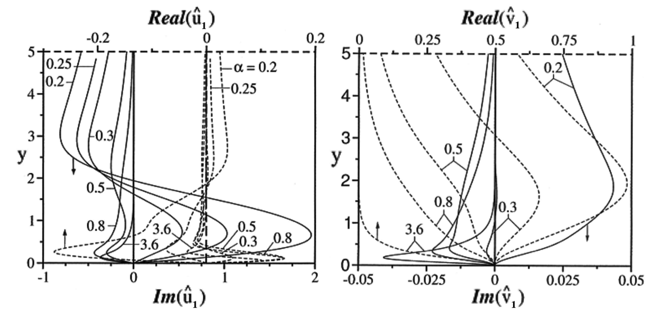

a) b)

Fig. 5 Flow modifications induced by the nonuniform suction with the Reynolds number $Re = 10^3$ as a function of the suction wave number α: a) $\hat{u}_1(y)$ and b) $\hat{v}_1(y)$. Solid and dashed lines represent imaginary and real parts, respectively. All results are normalized with $S = 1$. The presented results are for the Falkner–Skan boundary layer with $\beta = -0.07$ and $\gamma = 0$.

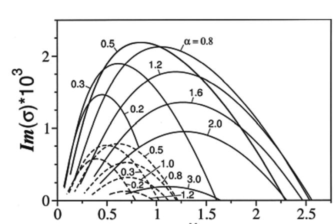

Fig. 6 Variations of the amplification rates $\mathrm{Im}(\sigma)$ of disturbances in the form of streamwise vortices as a function of the spanwise vortex wave number μ. The amplitude of the suction nonuniformities is $S = 0.006$. Dashed and solid lines correspond to $Re = 10^3$ and 2×10^3, respectively. The presented results are for the Falkner–Skan boundary layer with $\beta = -0.07$ and $\gamma = 0$.

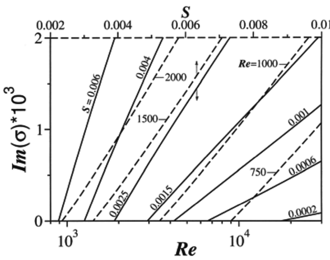

Fig. 7 Variations of the amplification rates $\mathrm{Im}(\sigma)$ of disturbances in the form of streamwise vortices as a function of the amplitude S of the suction nonuniformities for different levels of the flow Reynolds number (dashed lines). Also, variations of the amplification rates $\mathrm{Im}(\sigma)$ as a function of the flow Reynolds number for different levels of the amplitude S of suction nonuniformity (solid lines). The displayed results are for the streamwise vortices, with the wave number $\mu = 1.0$ induced by suction with the wave number $\alpha = 0.8$ for the Falkner–Skan boundary layer with $\beta = -0.07$ and $\gamma = 0$.

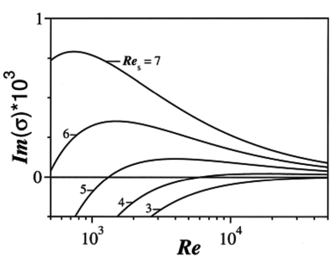

Fig. 8 Variations of the amplification rates $\mathrm{Im}(\sigma)$ of disturbances in the form of streamwise vortices as a function of the flow Reynolds number for different levels of Re_s. The displayed results are for the streamwise vortices with the wave number $\mu = 1.0$ induced by the suction with the wave number $\alpha = 0.8$ for the Falkner–Skan boundary layer with $\beta = -0.07$ and $\gamma = 0$.

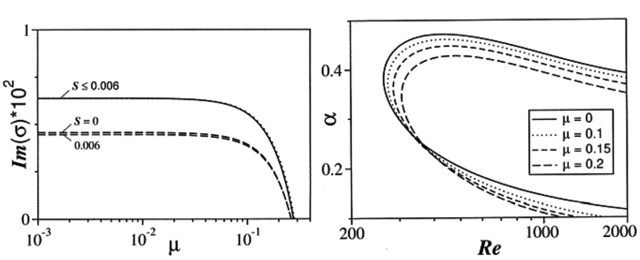

a) b)

Fig. 9 Stability characteristics of oblique TS waves: a) variations of the amplification rates $\mathrm{Im}(\sigma)$ as a function of the spanwise wave number μ [results are shown for the suction wave number $\alpha = 0.38$ and for the suction amplitude $S = 0.006$ for $Re = 400$ (dashed lines) and $Re = 600$ (solid lines); selected wave number corresponds approximately to the critical value in the absence of suction nonuniformities] and b) neutral curves for four types of oblique TS waves (those with $\mu = 0, 0.1, 0.15, 0.2$). All results given are for the Falkner–Skan boundary layer with $\beta = -0.07$ and $\gamma = 0$.

2. *Instability in the Form of Traveling Waves*

Figure 9a displays amplification rates for oblique TS waves computed at $Re = 400$ and 600 for the amplitude of suction nonuniformity varying over the range $0 \leq S \leq 0.006$. It can be seen that the amplification rates are initially fairly constant and then begin to decrease abruptly as the spanwise wave number increases. The amplitude of the suction nonuniformity has little effect on the instability over the entire range of the spanwise wave numbers and suction amplitudes considered. An increase of the Reynolds number leads to a modest increase of the amplification rate. Figure 9b displays neutral curves for oblique TS waves with various spanwise wave numbers μ. Purely two-dimensional TS waves corresponding to $\mu = 0$ are seen to be the most dangerous. There is a small decrease of the critical TS wave number from $\alpha \approx 0.38$ to ≈ 0.34 as the level of obliqueness is increased from $\mu = 0$ to 0.2, respectively. It can be concluded that the two-dimensional TS waves remain the most dangerous whether or not suction nonuniformities are present.

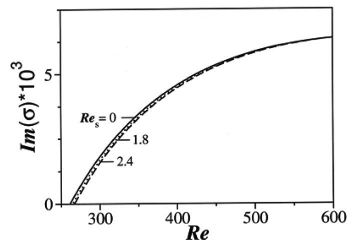

Fig. 10 Variations of amplification rates $\mathrm{Im}(\sigma)$ of two-dimensional TS waves as a function of the flow Reynolds number for the suction wave number $\alpha = 0.38$ for different values of Re_s. The wave number selected corresponds approximately to the critical value in the absence of suction nonuniformities. The presented results are for the Falkner–Skan boundary layer with $\beta = -0.07$ and $\gamma = 0$.

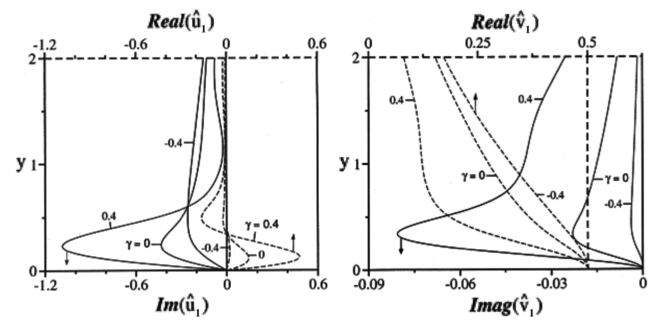

a) b)

Fig. 11 Variation of the flow modifications induced by the suction nonuniformities with the wave number $\alpha = 0.8$ for the flow Reynolds number $Re = 10^3$ for different values of the suction parameter γ: a) $\hat{u}_1(y)$ and b) $\hat{v}_1(y)$. The presented results are for the Falkner–Skan boundary layer with $\beta = -0.07$. Solid and dashed lines represent imaginary and real parts, respectively. All results are normalized with $S = 1$.

Figure 10 demonstrates that two-dimensional TS waves are weakly stabilized by suction nonuniformity. This effect becomes negligible as the Reynolds number is increased. Overall, small suction nonuniformities are shown to have a small effect on the TS waves.

B. Boundary Layer with Uniform Suction/Blowing ($\gamma = -0.4, 0.4$)

Results discussed in Section V.A indicate that suction nonuniformities induce instability in the form of streamwise vortices and have only a minimal effect on instability in the form of TS waves. The purpose of this section is to describe the instability of decelerated boundary layers modified by either uniform suction or uniform blowing. In particular, we shall inquire whether the application of uniform suction is an effective tool for flow stabilization when suction nonuniformities are present.

Figure 3 displays Falkner–Skan velocity profiles corresponding to suction parameter $\gamma = -0.4$ and $+0.4$. The form of these profiles illustrates the effects of uniform suction/blowing on the mean velocity distribution.

Figure 11 illustrates the form of velocity modifications that are induced by suction nonuniformities. It may be noted that the flow modifications for the case of uniform blowing (suction) are larger (smaller) than those found for the case of no uniform suction/blowing (i.e., $\gamma = 0$). Thus, individual modified mean flows differ substantially depending on whether uniform blowing or suction is

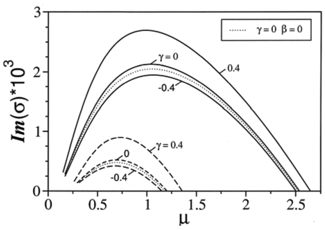

Fig. 12 Variations of the amplification rates $\mathrm{Im}(\sigma)$ as a function of the spanwise wave number μ for disturbances in the form of streamwise vortices induced by the suction nonuniformities with the wave number $\alpha = 0.8$ and amplitude $S = 0.006$ for uniform suction $\gamma = -0.4$, 0, and $+0.4$. Dashed and solid lines correspond to $Re = 10^3$ and 2×10^3, respectively. The presented results are for the Falkner–Skan boundary layer with $\beta = -0.07$. Results for the Blasius boundary layer are shown for reference purposes.

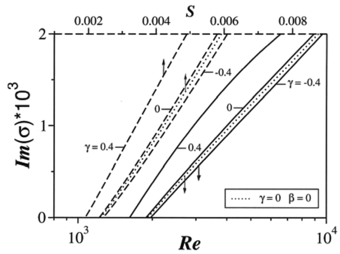

Fig. 13 Variations of the amplification rates $\mathrm{Im}(\sigma)$ of disturbances in the form of streamwise vortices as a function of the amplitude S of suction nonuniformities for uniform suction $\gamma = -0.4$, 0, and $+0.4$ for the flow Reynolds number $Re = 2 \times 10^3$ (dashed lines). Also, variations of the amplification rates $\mathrm{Im}(\sigma)$ as a function of the flow Reynolds number for uniform suction $\gamma = -0.4$, 0, and $+0.4$ with the suction amplitude $S = 0.0025$ (solid lines). The displayed results are for the streamwise vortices with $\mu = 1.0$, suction nonuniformities with the wave number $\alpha = 0.8$, and Falkner–Skan boundary layer with $\beta = -0.07$. Results for the Blasius boundary layer are shown for reference purposes.

involved. It should be noted that although the uniform suction/blowing is designated by $\gamma = \text{const}$, this does not correspond precisely to suction/blowing being constant in the streamwise direction. Rather, the rate of suction variations in the streamwise direction is similar to the rate of boundary-layer growth and thus may be neglected in the analysis.

1. Instability of the Form of Streamwise Vortices

Figure 12 provides a comparison of amplification rates for disturbances in the form of streamwise vortices induced by suction nonuniformity with amplitude $S = 0.006$ and streamwise wave number $\alpha = 0.8$. Two different Reynolds number are considered ($Re = 10^3$ and 2×10^3), as well as three different levels of uniform suction ($\gamma = -0.4$, 0, $+0.4$). The results for the Blasius boundary layer are shown for reference purposes. Further inspection of Fig. 12 reveals that amplification rates appear to be weakly dependant on the amount of uniform suction/blowing applied. The uniform suction slightly stabilizes the flow, whereas the blowing destabilizes it, with the blowing effect being stronger. Thus, flows with adverse pressure gradient appear to be only marginally less stable than flows without pressure gradient. In summary, the addition of large uniform suction/blowing and/or adverse pressure gradient is seen to produce only weak changes in the instability characteristics.

Figure 13 demonstrates that amplification rates significantly increase when either the Reynolds number or the amplitude of suction nonuniformity is increased. These results also illustrate that the instability is little affected by either the application of large uniform blowing ($\gamma = +0.4$) or large uniform suction ($\gamma = -0.4$). Comparison with the results for the Blasius boundary layer shows that the instability is little affected by changes in the pressure gradient.

Figure 14 illustrates the variation of amplification rates as a function of Reynolds number for two values of constant suction Reynolds number Re_s. It appears that amplification rates reach an asymptotic value for high values of Re and thus permit identification of critical conditions. The value of suction Reynolds number that guarantees flow stability, in the range of parameters considered, changes from $Re_s \approx 3$ for uniform suction with $\gamma = -0.4$ to a lesser value of $Re_s \approx 1$ for blowing with $\gamma = +0.4$. It can also be seen that uniform blowing has a larger effect on the flow than uniform suction, but overall such effects are still small.

2. Instability in the Form of Traveling Waves

Figure 15 displays the stability characteristics of oblique TS waves in the Falkner–Skan flows with either uniform wall suction ($\gamma = -0.4$) or uniform wall blowing ($\gamma = +0.4$). For the case of uniform blowing, the results indicate that two-dimensional TS waves are the most unstable. The amplification rates for flows with uniform blowing are two orders of magnitude greater than for flows with uniform suction and appear to depend very weakly on the amplitude of suction nonuniformities in the range of parameters considered. In contrast, the strength of the instability of flows involving uniform

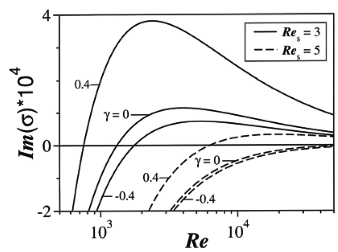

Fig. 14 Variations of the amplification rates $\mathrm{Im}(\sigma)$ of disturbances in the form of streamwise vortices as a function of the flow Reynolds number for $Re_s = 5$ and 3. Displayed results are for streamwise vortices with $\mu = 1.0$ and $\alpha = 0.8$ for uniform suction $\gamma = -0.4$, 0, and $+0.4$ for the Falkner–Skan boundary layer with $\beta = -0.7$.

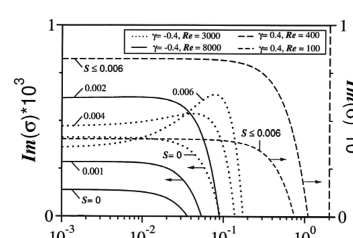

Fig. 15 Variations of the amplification rates $\mathrm{Im}(\sigma)$ of oblique TS waves as a function of the spanwise wave number μ for different values of the amplitude S of suction nonuniformities. Results are given for the Falkner–Skan boundary layer with $\beta = -0.07$ for uniform suction, corresponding to $\gamma = -0.4$ and $Re = 3000$ and 8000, and for uniform blowing, corresponding to $\gamma = +0.4$ and $Re = 100$ and 400. The wave numbers selected correspond approximately to the critical values in the absence of suction nonuniformities (i.e., $\alpha = 0.21$ in the former case and $\alpha = 0.77$ in the latter case).

wall suction varies widely with the level of suction nonuniformity. It can be seen that, in this case, the oblique waves are the most dangerous.

Figure 16 displays neutral curves for the TS waves with different levels of obliqueness. It can be seen that in the case of flow with uniform blowing, the two-dimensional waves are the most dangerous, whereas in the case of flows with uniform suction, the oblique waves become the most dangerous.

Figure 17 compares stability characteristics of two-dimensional TS waves using Re_s as a measure of the strength of suction nonuniformities. The amplification rates for flows with uniform blowing are seen to be approximately two orders of magnitude greater than amplification rates for flows with uniform suction. These amplification rates are almost unaffected by suction nonuniformities

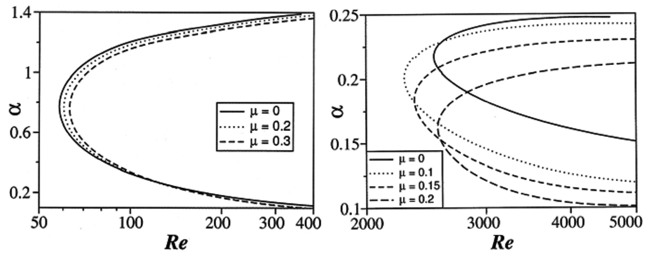

a) b)

Fig. 16 The neutral stability curves describing oblique TS waves in a Falkner–Skan boundary layer with $\beta = -0.07$ modified by suction nonuniformities with amplitude $S = 0.006$: a) boundary layer with uniform blowing $\gamma = +0.4$ and b) boundary layer with uniform suction $\gamma = -0.4$.

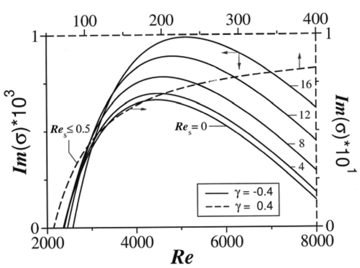

Fig. 17 Variations of the amplification rate $\mathrm{Im}(\sigma)$ of two-dimensional TS waves as a function of the flow Reynolds number for different values of Re_s for uniform suction corresponding to $\gamma = -0.4$ and uniform blowing corresponding to $\gamma = +0.4$. The wave numbers selected correspond approximately to the critical values in the absence of suction/blowing nonuniformities (i.e., $\alpha = 0.21$ in the former case and $\alpha = 0.77$ in the latter case). The presented results are for the Falkner–Skan boundary layers with $\beta = -0.07$.

in the case of uniform blowing ($\gamma = +0.4$) in the range of the suction Reynolds numbers subject to the investigation (i.e., for $Re_s \leq 0.5$). The amplification rates are, however, a very strong function of suction nonuniformities for flows modified by uniform suction. The reader may note that the need to use largely different values of Re_s in the case of uniform blowing and uniform suction is dictated by the fact that the critical Reynolds numbers differ in both cases by an order of magnitude.

VI. Conclusions

The linear stability of boundary layers with an adverse pressure gradient modified by nonuniformities of surface suction was investigated. Boundary layers were represented as self-similar Falkner–Skan flows with pressure parameter $\beta = -0.07$ and uniform suction/blowing parameter $\gamma = -0.4$, 0, +0.4. Arbitrary distributions of suction nonuniformities were represented in terms of the Fourier series. Detailed calculations were carried out for the suction nonuniformity in the form of a cosine function with amplitude S and wave number α.

The available results showed that two types of instability are possible. The first one involves the traveling TS (Tollmien–Schlichting) waves that are little modified by the presence of suction nonuniformities. The second one involves streamwise vortices that arise only because of the presence of the nonuniformities. This instability can be induced by a finite band of suction wave numbers. Each particular suction wave number gives rise to a finite band of unstable vortex (spanwise) wave numbers. The strength of the instability increases almost linearly with the amplitude of the suction nonuniformities and the flow Reynolds number in the range of parameters studied. The instability does not occur if the suction Reynolds number is $Re_s < 3$. Application of uniform suction has a small stabilizing effect.

The vortex instability is found to occur at Reynolds numbers that are an order of magnitude greater than the Reynolds numbers required to induce the TS instability. When uniform wall suction is applied, the critical Reynolds number for the TS instability is reduced, and when sufficiently high suction is used, the vortex instability may become the principle instability.

Nonuniformities in surface blowing induce an instability similar to that induced by the surface suction. The characteristics of this instability are very similar to the characteristics of the suction-induced instability.

Appendix: Linear Disturbance Equations

$$
\begin{aligned}
&T^{(m)}(t_m g_w^{(m)} - \mu g_u^{(m)}) + Re\mu D u_0 g_v^{(m)} \\
&\quad = iRe(N_u^{(m)} g_u^{(m-1)}) + N_w^{(m)} g_w^{(m-1)} + N_v^{(m)} g_v^{(m-1)} \\
&\quad + K_u^{(m)} g_u^{(m+1)} + K_w^{(m)} g_w^{(m+1)} + K_v^{(m)} g_v^{(m+1)})
\end{aligned} \tag{A1}
$$

$$
\begin{aligned}
&S^{(m)} g_v^{(m)} = -Re(L_u^{(m)} g_u^{(m-1)} + L_w^{(m)} g_w^{(m-1)} + L_v^{(m)} g_v^{(m-1)} \\
&\quad + M_u^{(m)} g_u^{(m+1)} + M_w^{(m)} g_w^{(m+1)} + M_v^{(m)} g_v^{(m+1)})
\end{aligned} \tag{A2}
$$

$$
it_m g_u^{(m)} + i\mu g_w^{(m)} + D g_v^{(m)} = 0 \tag{A3}
$$

where

$$
D = \mathrm{d}/\mathrm{d}y, \qquad t_m = \delta + m\alpha, \qquad k_m^2 = t_m^2 + \mu^2,
$$
$$
T^{(m)} = D^2 - k_m^2 - iRe(t_m u_0 - \sigma)
$$

$$
S^{(m)} = (D^2 - k_m^2)^2 - iRe(t_m u_0 - \sigma)(D^2 - k_m^2) + iRe t_m D^2 u_0
$$

$$
N_u^{(m)} = -\mu t_m \hat{u}_1 + i\mu \hat{v}_1 D, \qquad N_w^{(m)} = (t_m^2 - \alpha t_m)\hat{u}_1 - it_m \hat{v}_1 D
$$
$$
N_v^{(m)} = i\mu D\hat{u}_1
$$

$$
K_u^{(m)} = \mu(-t_m \hat{u}_1^* + i\hat{v}_1^* D), \qquad K_w^{(m)} = (\mathrm{t}_m^2 + \alpha t_m)\hat{u}_1^* - it_m \hat{v}_1^* D
$$
$$
K_v^{(m)} = i\mu D\hat{u}_1^*
$$

$$
L_u^{(m)} = -t_m^2 D\hat{u}_1 + i\alpha k_m^2 \hat{v}_1 + t_m(-t_m \hat{u}_1 + iD\hat{v}_1)D + it_m \hat{v}_1 D^2
$$

$$
L_w^{(m)} = \mu[-t_m D\hat{u}_1 + \alpha D\hat{u}_1 + (-t_m \hat{u}_1 + \alpha \hat{u}_1 + iD\hat{v}_1)D + i\hat{v}_1 D^2]
$$

$$
L_v^{(m)} = it_m D^2 \hat{u}_1 + k_m^2 D\hat{v}_1 + it_{m-1} k_m^2 \hat{u}_1 + (it_m D\hat{u}_1 + k_m^2 \hat{v}_1)D
$$

$$
M_u^{(m)} = -t_m^2 D\hat{u}_1^* - i\alpha k_m^2 \hat{v}_1^* + t_m(-t_m \hat{u}_1^* + iD\hat{u}_1^*)D + it_m \hat{v}_1^* D^2
$$

$$
M_w^{(m)} = \mu[-t_m D\hat{u}_1^* - \alpha D\hat{u}_1^* + (-t_m \hat{u}_1^* - \alpha \hat{u}_1^* + iD\hat{v}_1^*)D + i\hat{v}_1^* D^2]
$$

$$
M_v^{(m)} = it_m D^2 \hat{u}_1^* + k_m^2 D\hat{v}_1^* + it_{m+1} k_m^2 \hat{u}_1^* + (it_m D\hat{u}_1^* + k_m^2 \hat{v}_1^*)D
$$

and asterisks denote complex conjugate.

Acknowledgment

This work was carried out with the support of the Natural Sciences and Engineering Research Council (NSERC) of Canada, Canadair, and de Haviland Inc.

References

[1] Schlichting, H., *Boundary Layer Theory*, 7th ed., McGraw–Hill, New York, 1979.

[2] Reed, H. L., and Nayfeh, A. H., "Numerical-Perturbation Technique for Stability of Flat Plate Boundary Layers with Suction," *AIAA Journal*, Vol. 24, No. 2, 1986, pp. 208–214.

[3] MacManus, D. G., and Eaton, J. A., "Flow Physics of Discrete Boundary Layer Suction—Measurements and Predictions," *Journal of Fluid Mechanics*, Vol. 417, 2000, pp. 45–75.

[4] Schmid, P. J., and Henningson, D. S., *Stability and Transition in Shear Flows*, Applied Mathematical Sciences, Vol. 142, Springer, New York, 2001.

[5] Reed, H., Saric, W. S., and Arnal, D., "Linear Stability Theory Applied to Boundary Layers," *Annual Review of Fluid Mechanics*, Vol. 28, 1996, pp. 389–428.
doi:10.1146/annurev.fl.28.010196.002133

[6] Andersson, P., Brandt, L., Bottaro, A., and Hennigson, D. S., "On the Breakdown of Boundary Layer Streaks," *Journal of Fluid Mechanics*, Vol. 428, Feb. 2001, pp. 29–60.
doi:10.1017/S0022112000002421

[7] Andersson, P., Berggren, M., and Henningson, D. S., "Optimal Disturbances and Bypass Transition in Boundary Layers," *Physics of Fluids*, Vol. 11, Jan. 1999, pp. 134–150.
doi:10.1063/1.869908

[8] Corbett, P., and Bottaro, A., "Optimal Perturbations for Boundary Layers Subject to Streamwise Pressure Gradient," *Physics of Fluids*, Vol. 12, Jan. 2000, pp. 120–130.
doi:10.1063/1.870287

[9] Tumin, A., "A Model of Spatial Algebraic Growth in a Boundary Layer Subjected to a Streamwise Pressure Gradient," *Physics of Fluids*, Vol. 13, No. 5, 2001, pp. 1521–1523.
doi:10.1063/1.1361094

[10] Cathalifaud, P., and Luchini, P., "Algebraic Growth in Boundary Layers: Optimal Control by Blowing and Suction at the Wall," *European Journal of Mechanics, B/Fluids*, Vol. 19, July 2000, pp. 469–478.
doi:10.1016/S0997-7546(00)00128-X

[11] Floryan, J. M., "Stability of Wall-Bounded Shear Layers in the Presence of Simulated Distributed Surface Roughness," *Journal of Fluid Mechanics*, Vol. 335, Mar. 1997, pp. 29–55.
doi:10.1017/S0022112096004429

[12] Floryan, J. M., "Instability of Boundary Layers in the Presence of Weak Distributed Surface Suction," *Canadian Aeronautics and Space Journal*, Vol. 47, No. 4, 2001, pp. 367–371.

[13] Roberts, P. J. D., Floryan, J. M., Casalis, G., and Arnal, D., "Boundary Layer Instability Induced by Wall Suction," *Physics of Fluids*, Vol. 13, Sept. 2001, pp. 2543–2553.
doi:10.1063/1.1384868

[14] Roberts, P. J. D., and Floryan, J. M., "Instability of Accelerated Boundary Layers Induced by Surface Suction," *AIAA Journal*, Vol. 40, No. 5, May 2002, pp. 851–859.

[15] Biringen, S., "Active Control of Transition Using Suction-Blowing," *Physics of Fluids*, Vol. 27, June 1984, pp. 1345–1347.
doi:10.1063/1.864774

[16] Szumbarski, J. and Floryan, J. M., "Forcing of Channel Flow Using Distributed Suction—A Linear Theory," Expert Systems in Fluid Dynamics Research Lab., Dept. of Mechanical and Materials Engineering, Univ. of Western Ontario, Rept. ESFD-1/99, London, Ontario, Canada, 1999.

[17] Floryan, J. M., "Three-Dimensional Instabilities of Laminar Flow in a Rough Channel and the Concept of Hydraulically Smooth Wall," *European Journal of Mechanics, B/Fluids*, Vol. 26, No. 3, May–June 2007, pp. 305–329.
doi:10.1016/j.euromechflu.2006.07.002

[18] Klingman, B. G. B., Boiko, A. V., Westin, K. J. A., Kozlov, V. V., and Alfredsson, P. H., "Experiments on Stability of Tollmien-Schlichting Waves," *European Journal of Mechanics, B/Fluids*, Vol. 12, No. 4, July–Aug. 1993, pp. 493–514.

[19] Casalis, G., "Instabilite Secondaire de la Couche Limite Laminaire Tridimensionelle en Ecoulement Incompressible: Description du Code de Calcul," Rept.. 63/5618.54, Dept. d'Aerothermodynamique, Centre d'Etudes et de Recherches de Toulouse, ONERA, Toulouse, France, 1991.

[20] Coddington, E. A., and Levinson, N., *Theory of Ordinary Differential Equations*, McGraw–Hill, New York, 1965.

A. Tumin
Associate Editor